arXiv:1601.07350v1 [cond-mat.mes-hall] 27 Jan 2016

Ab-initio investigation of structural, electronic, and optical properties of (5,0) finite-length carbon nanotube

Mahdi Tarighi Ahmadpour,[1] S. Javad Hashemifar,[2] and Ali Rostamnejadi[1]

[1] *Electroceram research center, Malek Ashtar University of Technology, Shahinshahr, Isfahan, Iran*
[2] *Department of Physics, Isfahan University of Technology, 84156-83111 Isfahan, Iran*[*]

(Dated: January 28, 2016)

We use density functional computations to study the size effects on the structural, electronic, magnetic, and optical properties of (5,0) finite carbon nanotubes (FCNT), with length in the range of 4-44 Å. It is found that the structural and electronic properties of (5,0) FCNTs, in the ground state, converge at a length of about 30 Å, while the excited state properties exhibit long-range edge effects. We discuss that curvature effects govern the electronic structure of short (5,0) FCNTs and enhance energy gap of these systems, in contrast to the known trend in the periodic limit. It is seen that compensation of curvature effects in two special small sizes, may give rise to spontaneous magnetization. The obtained cohesive energies provide some insights into the effects of environment on the growth of FCNTs. The second-order difference of the total energies reveals an important magic size of about 15 Å. The optical and dynamical magnetic responses of the FCNTs to polarized electromagnetic pulses are studied by time dependent density functional theory. The obtained results show that the static and dynamic magnetic properties mainly come from the edge carbon atoms. The optical absorption properties are described in term of local field effects and characterized by Casida linear response calculations.

I. INTRODUCTION

Recently, finite-length carbon nanotubes (FCNTs) are of vast interest due to their potential applications in enhanced light emitting,[1] spintronics designing,[2,3] spin-orbit interaction based optoelectronic,[4] and heterojunction nanoelectronic devices.[5,6] It has been found that the electronic properties of sub-nanometer length FCNTs differ substantially from those of periodic CNTs, because of the alternation of electronic structure from one-dimensional to the zero-dimensional characteristic.[7–9] This fact implies that energy states of FCNTs are strictly affected by the length[10–12] and the edge structure of the tube.[13–15] For example, while periodic armchair CNTs represent a metallic character, finite armchair CNTs exhibit an energy gap which decreases periodically toward zero by increasing the length. In the case of zigzag CNTs the situation is different. On one hand, periodic zigzag CNTs can be either metal or semiconductor, depending on their chiral angle. On the other hand, electronic structure of finite zigzag CNTs are dominated by some localized edge states, which are evidenced by scanning tunneling spectroscopy of graphite[16] and may induce spin-polarization in the system.[15,17]

Thermodynamic considerations suggest that (5,0) CNT is the narrowest feasible zigzag carbon nanotube.[18] Because of its high curvature, the electronic properties of this nanotube is more complicated than the larger zigzag nanotubes.[8] The well-known $\sigma^*-\pi^*$ rehybridization, as a consequence of this high curvature, forces the zone-folded semiconducting band gap of periodic (5,0) CNT to close.[19,20] While periodic structure of this tube is extensively studied,[20–24] there is no systematic study about finite size effects on the physical properties of this system. Moreover, first-principles studies on FCNTs are mainly limited to the ground state properties and understanding finite size effects on the excited states properties of these systems demands further theoretical investigations.

The dependence of electronic and optical properties of FCNTs on their geometric features is promising to design flexible and sensitive optoelectronic and spintronics devices. The specific aim of this study is to investigate length-dependent structural, electronic, magnetic and optical properties of (5,0) FCNTs by using static and time dependent first-principles calculations.

II. METHODS

The ground state calculations were performed within the Kohn-Sham density functional theory (DFT) at the scalar relativistic limit, by using the local density (LDA)[25] and local spin density approximations (LSDA) implemented in the full-potential `FHI-aims` code.[26] The studied finite nanotubes were terminated by sufficient number of hydrogen atoms to saturate their edge dangling bonds. Full structural relaxations were applied to the systems down to the residual atomic forces of less than 10^{-3} eV/Å. The carbon and hydrogen atoms were treated tightly in the calculations. The length of the tubes throughout this paper is described in unit of a 0.2 nm thick structural section along the tube axis (Fig. 1a). The FCNTs are tagged by Si, where i denotes the number of sections of the system.

The optical absorption spectra were evaluated in the framework of time dependent DFT (TDDFT) and pseudopotential technique, implemented in computer package `Octopus`.[27] The TDDFT approach has already been used for successful interpretation of the excited states properties of a (7,6) FCNT.[28] We used norm-conserving pseudopotentials in the form of Troullier-Martins and time-dependent LDA (TD-LDA) kernel.[29] It is already dis-

cussed that TD-LDA is able to provide reliable results for finite systems.[30] In `Octopus`, the ground state density is evaluated over a discrete grid in real space. The radius of overlapping spheres around each atom and the grid spacing were optimized to 3.5 and 0.16 Å, respectively. Electric dipole response (optical absorption) of the systems are calculated by explicit real time-propagation of the Kohn-Sham wave functions,[31] in the presence of a weak white uniform electric pulse. To achieve a fine spectrum, nearly 13000 time-steps are taken for a total propagation time of 20 $\hbar$/eV. The frequency response is extracted via the Fourier transform of the time-dependent dipole moment. The Casida linear response approach was applied for characterization of the predicted optical transitions.[32] In order to evaluate the spin-dipole response of the FCNTs, opposite magnetic pulses were applied to the majority and minority spin channels.[33]

III. STRUCTURAL PROPERTIES

In this work we investigated the electronic structure and optical properties of finite length (5,0) carbon nanotubes composed of up to 22 sections. The atomic structure of S6, as a prototype, is depicted in Fig. 1a. The longitudinal and transverse bonds are denoted by L and T, respectively, and the bond angles are described by α and β. After full structural relaxation, these parameters are averaged over the central unit cell of the system and then plotted in Fig. 1b. It is expected that by increasing the tube length, the edge effects vanish and central unit cell acts as an infinite length periodic CNT. According to the figure, the L and T bond lengths, after almost 16 sections, converge to the values of about 1.40 and 1.44 Å, respectively, close to those reported for periodic (5,0) CNT.[20,23] For qualitative understanding of the hybridization in the systems, we compare these bond lengths with those of the ideal graphene (1.42 Å) and diamond (1.54 Å).[34]

The converged value of the longitudinal bond (1.40 Å) is smaller than the carbon-carbon bond in ideal graphene, while the converged value of the transverse bond (1.44 Å) has slightly increased toward the interatomic bond length in diamond. Hence, it seems that L bond has mainly a graphene like sp^2 hybridization, while T bond may involve a degree of sp^3 contribution.

The trends of α and β bond angles also confirm the presence of a remarkable sp^3 hybridization in the system. It is seen that α converges to a value of 111.2° (Fig. 1b), consistent with the sp^3 bond angle (109.5°), while β tends to a value of about 119.8°, which is close to the ideal sp^2 bond angle (120°).[34] It should be noted that the converged values of the bond angles coincide with the corresponding values in periodic (5,0) CNT.[20,23] The appearance of sp^3 hybridization in the systems comes from the significant curvature of the walls in such ultrathin CNTs.[35] In order to provide more insights into the curvature effects in (5,0) FCNTs, the highest occupied molecular orbital (HOMO), bond lengths, and bond angles of this system is compared with (7,0) and (9,0) finite tubes with the same length (table I). The diameter of (5,0), (7,0), and (9,0) CNTs are about 3.91, 5.48, and 7.05 Å, respectively. In the (9,0) tube, which has the largest diameter, the HOMO is seen to be localized on the edge atoms, while the wall curvature of smaller tubes pushes this orbital toward the central part of the system. Moreover, the bond lengths and bond angles of this

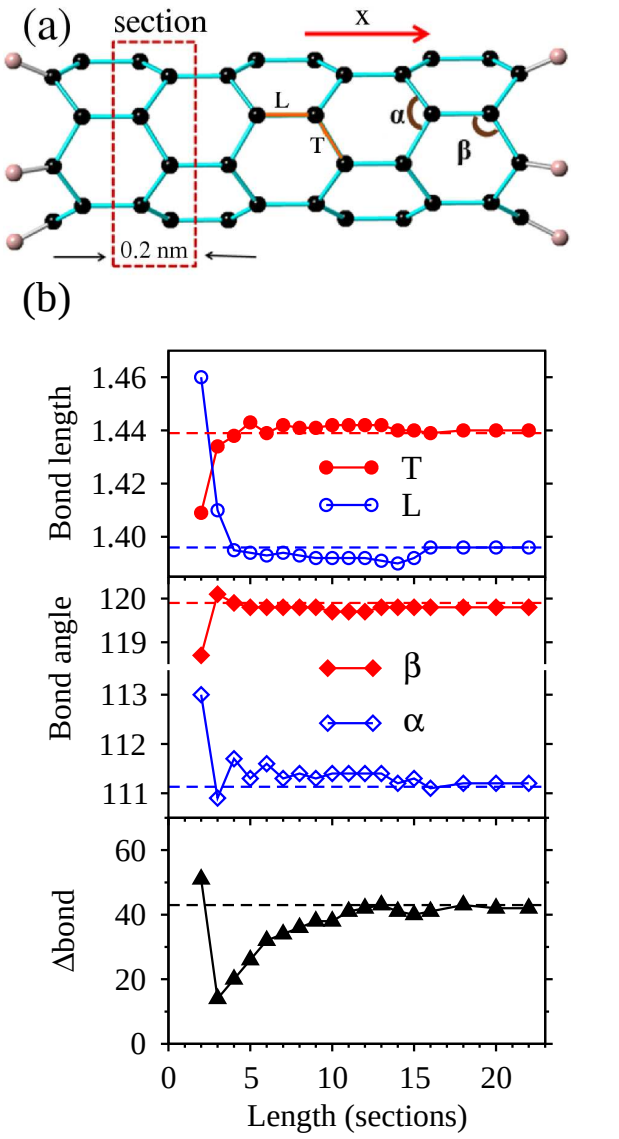

FIG. 1. (a): Schematic diagram of a finite length (5,0) carbon nanotube with 6 sections (S6). The dashed rectangle encloses a tube section. The longitudinal and transverse bonds are indicated by L and T, while α and β shows two investigated bond angles. (b): Variation of the L and T bond lengths (Å) and α and β bond angles (degree) versus the FCNT's length. The corresponding values for periodic nanotube (infinite-length) are indicated with dashed lines. Difference (Δbond) between the averaged L and T bond lengths over the entire of the tubes.

TABLE I. Comparing the highest occupied molecular orbital (HOMO) and structural parameters of three finite zigzag CNTs with the same lengths and different diameters. L, T, α, and β have the same meaning as in Fig. 1 and L_0 and α_0 are equilibrium bond length and bond angle in ideal graphene.[34]

FCNT	HOMO	L/L_0	T/L_0	α/α_0	β/α_0
(5,0)	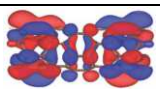	0.980	1.013	0.930	0.998
(7,0)	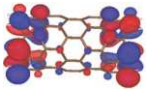	0.993	1.000	0.962	1.000
(9,0)	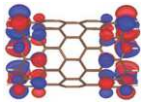	0.997	1.000	0.976	1.000

system are close to the corresponding parameters in the ideal graphene (table I), revealing the dominance of sp^2 hybridization in this system. In the smaller finite tubes, the curvature effects increase deviation of the bond parameters from the ideal graphene toward diamond, and thus enhance sp^3 hybridization in the systems.

In order to see the effects of passivation on structural properties of finite (5,0) CNTs, we tried to re-calculate some of the FCNTs in their pristine structure with no adsorbed hydrogen atoms. The presence of dangling bonds induces many difficulties in the self-consistent calculation of these unpassivated systems. After considerable efforts, we could only converge the self consistent electronic structure of S2, S3, and S4. It was found that, in contrast to the passivated CNTs, L bond becomes longer than T bond in these pristine FCNTs. It means that the unpassivated FCNTs have slightly longer length and narrower diameter, compared with the passivated ones. This slight elongation may be attributed to the non-bonded electrons of the pristine FCNTs that induce an effective repulsive force between the two ends of the system.

We observe that the size dependency of the structural parameters, presented in Fig. 1b, becomes negligibly small for tubes longer than S16. Therefore, one may omit the costly process of structural relaxation of longer (5,0) finite length carbon nanotubes by constructing their structure from the relaxed atomic configuration of S16. In order to verify this statement, we constructed the S18 tube from the structural parameters of S16 and then calculated its total energy and energy gap without and with a further structural relaxation. The same calculations were performed for S20 and S22 tubes and the results were listed in table II. It is clearly seen that the finite tubes longer than S16, constructed from the atomic configuration of smaller tubes, in practice need not any further structural relaxation for investigating their structural and electronic properties.

The cohesive energy of the systems as a function of the tube length is shown in Fig. 2. It is expected that by

TABLE II. Effect of a further structural relaxation on the total energy (ΔE_{tot}) and energy gap (Δgap) of a longer finite CNT constructed from the relaxed structure of the shorter tube.

	S14	S16	S18	S20	S22
ΔE_{tot}(Ry)	0.360	0.090	0.009	0.002	0.003
Δgap (Ry)	0.228	0.004	0.023	0.004	0.005

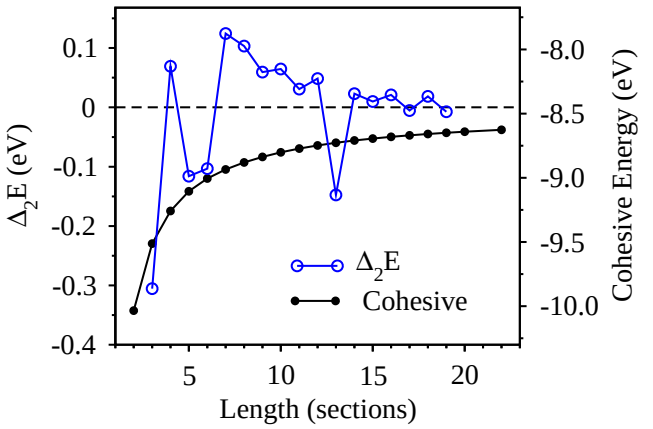

FIG. 2. Calculated cohesive energy (per carbon atom) and second energy difference ($\Delta_2 E$) of the (5,0) FCNTs. The dashed line shows the cohesive energy of the periodic tube.

increasing the tube length, the cohesive energy converges to the periodic limit (8.50 eV/atom). The absolute cohesive energy decreases as the length increases, indicating more stability of shorter tubes. It is attributed to the higher strength of C-H bond, compared with C-C bond. The shorter FCNTs have higher fractional number of C-H bonds and hence are more stable. Calculated harmonic vibrational frequencies of S2 and S3 provide further evidence for this statement; there is a very strong peak at about $3000\,cm^{-1}$ which is related to the C-H bond. Barone *et al.* observed similar behavior in graphene nanoribbons.[36] They discussed that the stability of the passivated nanoribbons is proportional to the molar fraction of hydrogen atom and therefore inversely proportional to the width of the system. In our case, the cohesive energy of FCNTs is inversely proportional to the tube length.

On the other hand, Rochefort *et al.* observed a reverse behavior,[37] their absolute cohesive energy of CNTs per atom increases as the length increases. This difference may be ascribed to the different energy reference used for calculation of cohesive energy in this work. Following some benchmark calculations, we realized that using a reference energy which includes C-H bond, like benzene or methane, give rises to a cohesive energy which decreases (become more negative) by increasing length. These statements may be helpful to identify the required experimental setup for synthesis of short or long FCNTs. It seems that in a high vacuum environment, long FCNTs

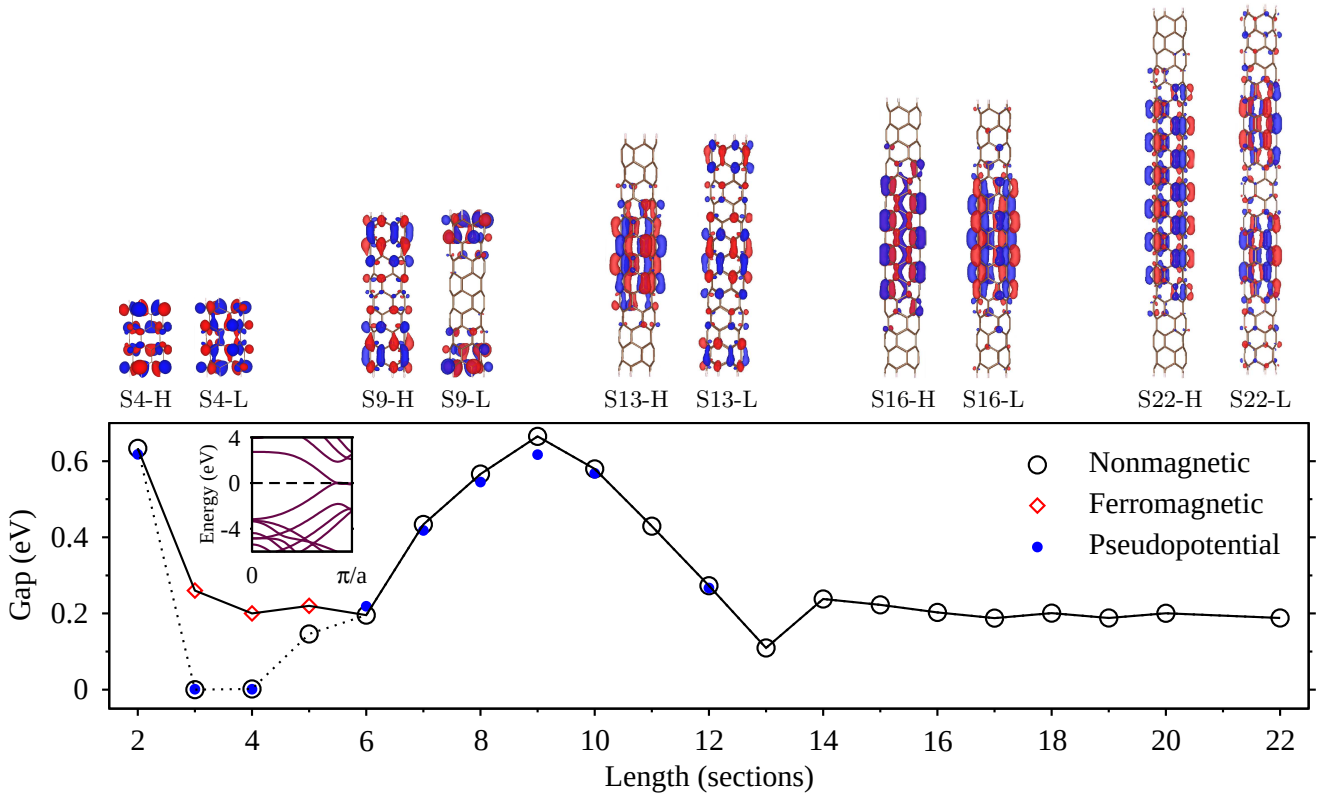

FIG. 3. Top: Isosurfaces of the highest occupied molecular orbital (HOMO) and the lowest unoccupied molecular orbital (LUMO) of (5,0) FCNTs with different length. Bottom: Calculated energy gap of the finite tubes as a function of the tube length. Inset: the electronic band structure of a graphene nanoribbon with a width of four sections.

are more feasible while production of short FCNTs may be more practical in the presence of a proper hydrogen gas flux.

In the study of atomic clusters, a conventional parameter for addressing relative stabilities is the second-order difference of total energy ($\Delta_2 E$), defined as:

$$\Delta_2 E(i) = E_{tot}(i+1) + E_{tot}(i-1) - 2E_{tot}(i) \qquad (1)$$

where $E_{tot}(i)$ denotes to the relaxed total energy of the cluster of size i. The positive values of this parameter determine the so called magic sizes of the system which exhibit higher stability with respect to the adjacent sizes. The second-order energy difference of the given FCNTs (Fig. 2) indicates that S7 and S8 are energetically the most favorable sizes, while S3, S5, S6, and S13 show the least relative stabilities. This plot is expected to be comparable with the envisaged mass spectra measurements on (5,0) FCNTs.

IV. ELECTRONIC PROPERTIES

The calculated energy gap of the finite CNTs, in the non-magnetic state, as a function of their length is represented in Fig. 3. In order to understand this behavior, one has to take into account the zone-folding and the curvature effects. The zone-folding approach is a popular method to estimate the electronic structure of a nanotube from its graphene counterpart. This approach predicts a semiconducting gap for infinite (3n±1,0) zigzag CNTs,[38] which in all cases larger than (5,0) CNT, agrees with the accurate DFT based calculations. The metallic behavior of the (5,0) CNT is attributed to the high curvature of this narrow tube, which is not taken into account in the zone-folding approach.[35,39] The high curvature of this system enhances the interatomic interactions and thus increases the dispersion of valence and conduction bands. Consequently, these bands overlap and form a metallic system. We will discuss that the curvature effects may have quite different impacts in the zone-folded electronic structure of the finite CNTs, which is derived from the electronic structure of graphene nano-ribbons (GNRs).

The electronic band structure of the GNR corresponding to S4, is calculated and presented in the inset of Fig. 3. It is seen that the valence and conduction bands are degenerate and flat near edge of the Brillouin zone (BZ). The width of the degenerate region increases by increasing the width of the GNR. Folding the GNR will discretize the allowed k-points of a (n,0) FCNT as: $k_N = \frac{2\pi}{a}\frac{N}{n}$ $(N = 0, \pm1, \pm2, \cdots)$ where a is the GNR lattice parameter.[17] For a (5,0) tube, five k-points satisfy the boundary condition, in which the last one falls on

the degenerate region and leaves a zero energy gap in the folded electronic structure of the systems. However, the obtained results (Fig. 3) indicate that all FCNTs, except S3 and S4, exhibit a non-trivial energy gap. The reason is that the high curvature of these finite systems enhances the interatomic interactions and consequently increases dispersion of the discrete energy levels to open a gap between the highest occupied (HOMO) and the lowest unoccupied (LUMO) levels. In other words, the curvature effects act oppositely in the finite and periodic CNTs; increasing band dispersion in a periodic CNT may give rise to overlapping of the valence and conduction bands, whereas increasing dispersion of discrete energy levels of a finite CNT may enhance the HOMO-LUMO splitting.

We use the difference between the average L and T bond lengths (Δbond), as a proper measure of the curvature of an FCNT. It is rationalized by the fact that this difference decreases toward zero by increasing the CNT diameter (table I). The results, presented in Fig. 1, indicate that in the smallest FCNT (S2), L bond is on average longer than T bond. By increasing the FCNT length, the L bond length falls quickly while the T bond length rises sharply. It is clearly observed that within S3 and S4 the longitudinal and transverse bond lengths are getting very close together. As a result, these systems involve the lowest curvature effects and hence their zero energy gap in the non-magnetic state agrees with the zone-folding prediction. On the other hand, S2 exhibits the highest curvature effect and consequently a significant energy gap appears in this system. We observe that from S4 to about S9, Δbond and consequently curvature are growing. This trend may explain the increment of energy gap between S4 and S9 (Fig. 3). For FCNTs longer than S9, Δbond is almost converged to the periodic CNT value and hence the curvature is saturated in this region. Therefore, the asymptotic decrease of the energy gap in this region should be explained by a different effect.

In larger FCNTs with lower curvature effect, similar asymptotic behavior, observed in a broad length range, is attributed to quantum confinement effects.[8] In the simple picture of *particle in a one-dimensional box*, the distance between quantum energy levels decreases asymptotically with respect to the box length. We observe that in the short (5,0) FCNTs, significant variation of curvature destroys the asymptotic behavior of the energy gap, while after stabilization of the curvature around S9, the asymptotic decrease of the quantum confinement appears (Fig. 3). However, the results show the decrease of energy gap stops around S15 and converges to a value of about 0.2 eV afterwards, whereas, the periodic (5,0) CNT has a metallic character within DFT. Therefore, long-range edge effects are expected in the electronic and optical spectra of (5,0) finite length CNTs. For better understanding of this behavior, the HOMO and LUMO isosurfaces of some investigated FCNTs are presented in the top of Fig. 3. It is apparent that the size dependency of HOMO is limited to the tubes shorter than S10, while for longer tubes this orbital exhibits a uniform distribution over the central sections of the FCNT. In contrast, LUMO exhibits persistent size dependent fluctuations even up to the size of S22 (44 Å). This observation provides more evidence for the resistant edge effects in the excited state properties of (5,0) FCNTs.

TABLE III. Calculated magnetic energy (ΔE), spin moment (μ), and spin density isosurfaces of some (5,0) FCNTs in the ferromagnetic state. The numbers in the parentheses show magnetic energy of the systems in the antiferromagnetic state.

FCNT	ΔE (meV)	μ (μ_B)	spin density
S3	-130 (0)	2.00	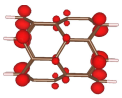
S4	-127 (-6)	2.00	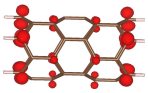
S5	0 (2)	2.00	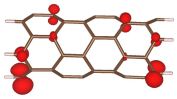

As it was mentioned earlier, the curvature of S3 and S4 is compensated and hence the zero energy gap of these systems is mainly derived from the zone-folding of the GNR sp^2 band structure. In other investigated FCNTs, the curvature effects play a significant role and induce a non-trivial sp^3 hybridization in the systems. In the case of sp^2 hybridization, the system has equivalent L and T bonds, just as graphene, while contribution of sp^3 hybridization in the systems with high curvature increases the length of the transverse T bond, compared with the longitudinal L bond, and opens a gap in the systems. This statement is justified by the behavior of Δbond in Fig. 1.

The zero energy gap of S3 and S4 zigzag FCNTs shows the potential of spontaneous spin polarization in the system. From a general point of view, the zigzag graphitic materials are predicted to possess a ferromagnetic (FM) or antiferromagnetic (AF) spin-polarized ground state.[40] Therefore, we studied the FM and AF states of the considered FCNTs within spin-polarized calculations. It was found that S3, S4, and S5 have FM and AF states (table III), while all other FCNTs exhibit no spontaneous spin polarization. The calculated spin densities reveal that the magnetic moment of S3, S4, and S5 is concentrated on the edge carbon atoms. The total spin moment of the spin-polarized systems is found to be $2\,\mu_B$, because there are two allowed k-points ($\pm 4\pi/5a$) in the degenerate region of the corresponding GNR band structure.

The magnetic energy of S3, S4, and S5 is also presented in table III. This parameter measures the difference between the minimized energy of system in the non-magnetic (NM) and corresponding magnetic states. We observe that S3 and S4 prefer a FM state which is significantly more stable than the NM and AF states. In the case of S5, the FM, AF, and NM state have very close

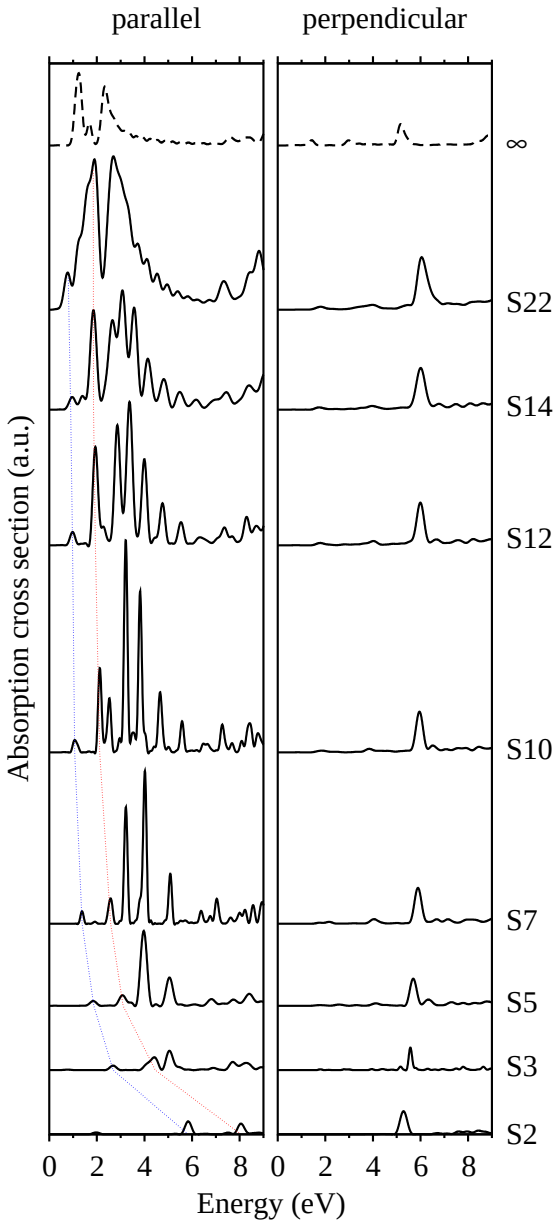

FIG. 4. Absorption cross section of the investigated FCNTs. The tube lengths are indicated in the right axis. The symbol ∞ stands for an infinite (periodic) (5,0) CNT. The evolution of the two first absorption peaks of the FCNTs are highlighted by the dotted and dashed lines.

minimized energies while the FM state is marginally more stable. We found that FM spin polarization has significant effect on the electronic structure of S3, S4, and S5. As it was expected, spin polarization removes the degeneracy of the HOMO and LUMO levels in S3 and S4 and opens a gap in these systems. The enhanced energy gap of these systems in the FM state is presented in Fig. 3. It should be noted that the minimized total energy of S3, S4, and S5, presented in Fig. 2 are determined in the FM state.

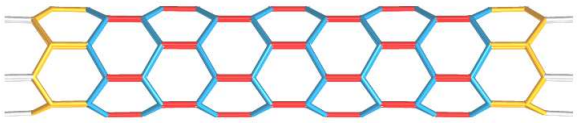

FIG. 5. Bond pattern of S10; red bonds are shorter than 1.40 Å, yellow bonds are between 1.40 and 1.44 Å, and blue bonds are longer than 1.44 Å.

V. OPTICAL SPECTRA

As it was mentioned, we used time dependent DFT to calculate absorption spectra of the desired finite CNTs in the presence of a polarized external electromagnetic field. The calculated absorption cross sections, for parallel and perpendicular polarization, are presented in Fig. 4. In the parallel polarization, the shorter tubes exhibit more sparse spectrum, originating from their discrete energy levels, while growing the tube length, increases the number of peaks and accumulates them together. It is due to the fact that by growing the tube length, the discrete energy states are getting more dense and gradually transforming to one dimensional bands. We observe that decreasing the tube length quenches the absorption intensities. This quenching is attributed to the local field effects (LFEs) or depolarization field emerged from microscopic electric dipoles induced by the external field. Fortunately, LFEs are well treated in the TDDFT formalism.[22] It is argued that the strength of LFEs decreases rapidly by increasing the relevant dimension of the system.[21] As a result, it is seen that growing the tube length significantly amplifies the absorption spectra in the parallel polarization, while fixed lateral dimension of FCNTs reduces the size sensitivity of the perpendicular absorption spectra. This lateral confinement give rises to strong perpendicular LFEs and hence quenches the absorption peaks in this polarization.

For better understanding of the absorption spectra in the parallel polarization, the behavior of the first two absorption peaks are highlighted by using two dashed lines in Fig. 4. The first dashed line (blue), which likely mimics trend of the optical gap of FCNTs, exhibits an obvious red shift, more pronounced in the shorter tubes. In other words, the optical gap of these systems is rapidly decreasing from S2 to S7 and then converging to the obtained optical band gap of periodic (5,0) tube ($\sim$1.2 eV). In contrast to our results, Montero *et al.* [11] observed a blue shift in the optical absorption of (5,0) FCNTs, computed using post Hartree-Fock method. Accurate inspection of their published paper shows that they have likely constructed their finite tubes by repeating the relaxed units of the periodic tube and no further structural relaxation has been applied to the finite systems. Our calculations indicate significant relaxation effects on edge atoms which affects the optical spectra of finite systems, specially for shorter tubes. The bond pattern of S10, as a prototype, is presented in Fig. 5.

TABLE IV. Character of the first allowed optical transition of S3, S5, S7, and S10 in the parallel and perpendicular polarizations. The capital letters L and H stand for LUMO and HOMO.

FCNT	parallel			perpendicular		
S3	H−2	→	L+4	H−15	→	L+5
S5	H−1	→	L+1	H−6	→	L+25
	H	→	L+4			
S7	H	→	L+6	H−9	→	L+20
				H−10	→	L+19
S10	H−2	→	L+5	H−39	→	L+14
				H−40	→	L+13
				H−42	→	L+16
				H−43	→	L+15

Compared with the electronic gap, presented in Fig. 3, optical gaps are significantly larger and display different trend. It may evidence absence of any HOMO-LUMO optical transition in the (5,0) FCNTs. In order to verify this statement, we used the linear response Casida approach to characterize the first allowed optical transitions of four FCNTs. The results, given in table IV, confirm absence of the HOMO-LUMO transition in the systems. In the case of S3 and S10, we observe that the first optical transition in the parallel polarization occurs from the second level below HOMO to the fourth and fifth levels above LUMO, respectively. In the case of S5, in the parallel polarization, and S7 and S10, in the perpendicular polarization, more than one joint levels was found to contribute to the first allowed optical transition. In the periodic CNTs, it is already discussed that the first allowed transition, in the parallel polarization, occurs between the valence and conduction bands which have identical orbital character.[41] Our results show that lack of translational symmetry changes the selection rules and hence prevents the HOMO-LUMO transition in the finite CNTs.

In the systems with spin polarized electronic structure, one may expect some magnetic responses to the photon (electromagnetic) irradiation, while non-magnetic systems exhibit only electric response to an external electromagnetic field.[42] Therefore, we calculated the spin dipole response of S3, S4, and S5 FCNTs to an external magnetic field, in the framework of TD-LSDA. The obtained spectra, presented in Fig. 6, illustrate stronger magnetic response of S3 and S4, likely due to their higher ferromagnetic energy, compared with S5 (table III). It is interesting to see that the higher responses of S3 and S4 happens in the visible spectrum. Comparing magnetic responses of the systems in the parallel and perpendicular polarizations shows that, in contrast to the electric responses, the effects of magnetic LFEs are not evident. The reason is that the magnetic moment of the systems, as it was mentioned earlier, is rather distributed over the edge

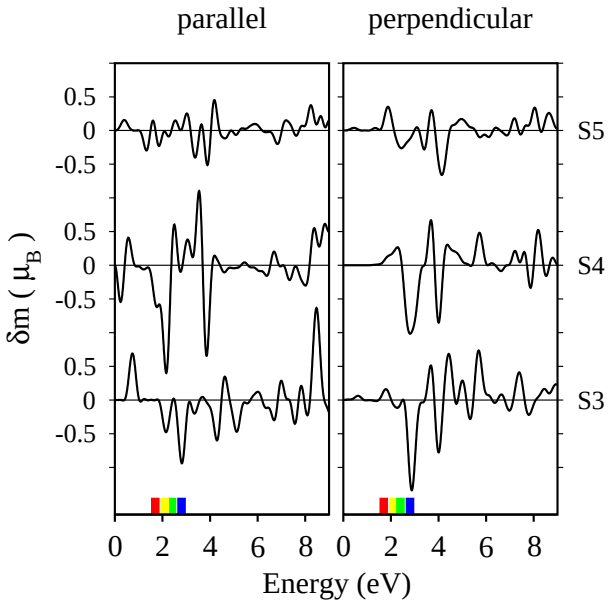

FIG. 6. Calculated dynamical spin dipole of S3, S4, and, S5. $\delta m(\omega) = \delta n^{\uparrow}(\omega) - \delta n^{\downarrow}(\omega)$ where $\delta n^{\uparrow(\downarrow)}(\omega)$ denotes the dynamical spin response of the system in the majority (minority) channel.[33] The energy range of the visible spectra is highlighted on the energy axes.

carbon atoms (see table III). As a result, the magnetic response mainly comes from the edge atoms and hence is less sensitive to the polarization. The interplay between optical excitations and dynamical magnetizations of FCNTs is promising to develop new nano devices for magneto-optical opportunities.

VI. CONCLUSIONS

In summary, full-potential density functional computations was employed to investigate structural and electronic properties of (5,0) finite carbon nanotubes (FCNTs), passivated with hydrogen atoms. The behavior of bond lengths and angles as a function of the tube length indicated that the ground state properties converge to the periodic limit at a length of about 30 Å. We discussed that the zone-folded electronic structure of the finite CNTs, in contrast to the periodic system, shows no energy gap, while high curvature of (5,0) FCNTs opens a gap in the system. It was argued that compensation of the curvature effects at a length of about 6-8 Å, preserves the sp^2 character of carbon-carbon bonds and closes the energy gap of FCNT in the nonmagnetic state, and then brings in a ferromagnetic state. Analysis of the second-order differences of total energy showed that for the (5,0) FCNTs shorter than 40 Å, a length of about 15 Åexhibits the highest relative stability. The behavior of the energy gap and the lowest unoccupied molecular orbital indicated that, in contrast to the ground state properties, the excited state properties of the systems exhibits

long range edge effects. The real time propagation of Kohn-Sham orbitals was applied to determine the electric dipole and spin dipole responses of FCNTs in the presence of electromagnetic pulses. The calculated optical absorption spectra show that the optical gap of the systems is considerably larger than the Kohn-Sham energy gap. The obtained character of optical transitions in the framework of Casida equation confirms absence of any optical transition between the highest unoccupied and the lowest unoccupied molecular orbitals in (5,0) finite CNTs. The spin dipole response of the systems, which is found to be more pronounced in the visible or near visible region, is of order of Bohr magneton.

VII. ACKNOWLEDGMENTS

We acknowledge the helpful comments of Mojtaba Alaei (Isfahan University of Technology).

* hashemifar@cc.iut.ac.ir

[1] Y. Miyauchi, M. Iwamura, S. Mouri, T. Kawazoe, M. Ohtsu, and K. Matsuda, Nat. Photon. **7**, 715719 (2013).
[2] A. Mañanes, F. Duque, A. Ayuela, M. J. López, and J. A. Alonso, Phys. Rev. B **78**, 035432 (2008).
[3] A. J. Du, Y. Chen, G. Q. Lu, and S. C. Smith, App. Phys. Lett. **93**, 073101 (2008).
[4] C. Galland and A. Imamoğlu, Phys. Rev. Lett. **101**, 157404 (2008).
[5] L. Chico, L. X. Benedict, S. G. Louie, and M. L. Cohen, Phys. Rev. B **54**, 2600 (1996).
[6] H. Santos, A. Ayuela, W. Jaskólski, M. Pelc, and L. Chico, Phys. Rev. B **80**, 035436 (2009).
[7] L. C. Venema, J. W. G. Wilder, H. L. J. T. Tuinstra, C. Dekker, A. G. Rinzler, and R. E. Smalley, App. Phys. Lett. **71**, 2629 (1997).
[8] H.-Y. Zhu, D. Klein, T. Schmalz, A. Rubio, and N. March, J. Phys. Chem. Solids **59**, 417 (1998).
[9] A. Rubio, D. Sánchez-Portal, E. Artacho, P. Ordejón, and J. M. Soler, Phys. Rev. Lett. **82**, 3520 (1999).
[10] R. A. Jishi, J. Bragin, and L. Lou, Phys. Rev. B **59**, 9862 (1999).
[11] A. L. Montero-Alejo, M. E. Fuentes, E. Menéndez-Proupin, W. Orellana, C. F. Bunge, L. A. Montero, and J. M. García de la Vega, Phys. Rev. B **81**, 235409 (2010).
[12] X. Sun, S. Zaric, D. Daranciang, K. Welsher, Y. Lu, X. Li, and H. Dai, J. Am. Chem. Soc. **130**, 6551 (2008).
[13] T. Yumura, K. Hirahara, S. Bandow, K. Yoshizawa, and S. Iijima, Chem. Phys. Lett. **386**, 38 (2004).
[14] J. Li, G. Zhou, L. Yang, J. Wu, and W. Duan, Phys. Rev. B **71**, 073409 (2005).
[15] J. Wu and F. Hagelberg, Phys. Rev. B **79**, 115436 (2009).
[16] Y. Niimi, T. Matsui, H. Kambara, K. Tagami, M. Tsukada, and H. Fukuyama, Phys. Rev. B **73**, 085421 (2006).
[17] S. Okada and A. Oshiyama, J. Phys. Soc. Jpn. **72**, 1510 (2003).
[18] M. López, I. Cabria, N. March, and J. Alonso, Carbon **43**, 1371 (2005).
[19] X. Blase, L. X. Benedict, E. L. Shirley, and S. G. Louie, Phys. Rev. Lett. **72**, 1878 (1994).
[20] M. Machón, S. Reich, C. Thomsen, D. Sánchez-Portal, and P. Ordejón, Phys. Rev. B **66**, 155410 (2002).
[21] C. D. Spataru, S. Ismail-Beigi, L. X. Benedict, and S. G. Louie, Phys. Rev. Lett. **92**, 077402 (2004).
[22] A. G. Marinopoulos, L. Reining, A. Rubio, and N. Vast, Phys. Rev. Lett. **91**, 046402 (2003).
[23] H. J. Liu and C. T. Chan, Phys. Rev. B **66**, 115416 (2002).
[24] E. Malić, M. Hirtschulz, F. Milde, A. Knorr, and S. Reich, Phys. Rev. B **74**, 195431 (2006).
[25] J. P. Perdew and A. Zunger, Phys. Rev. B **23**, 5048 (1981).
[26] V. Blum, R. Gehrke, F. Hanke, P. Havu, V. Havu, X. Ren, K. Reuter, and M. Scheffler, Comput. Phys. Commun. **180**, 2175 (2009).
[27] X. Andrade, D. Strubbe, U. De Giovannini, A. H. Larsen, M. J. T. Oliveira, J. Alberdi-Rodriguez, A. Varas, I. Theophilou, N. Helbig, M. J. Verstraete, L. Stella, F. Nogueira, A. Aspuru-Guzik, A. Castro, M. A. L. Marques, and A. Rubio, Phys. Chem. Chem. Phys. **17**, 31371 (2015).
[28] S. Tretiak, Nano Lett. **7**, 2201 (2007).
[29] E. K. U. Gross and W. Kohn, Phys. Rev. Lett. **55**, 2850 (1985).
[30] G. Onida, L. Reining, and A. Rubio, Rev. Mod. Phys. **74**, 601 (2002).
[31] K. Yabana and G. F. Bertsch, Phys. Rev. B **54**, 4484 (1996).
[32] M. E. Casida, "Time-dependent density functional response theory for molecules," in *Recent Advances in Density Functional Methods* (World Scientific, 2011) Chap. 5, pp. 155–192.
[33] M. B. Torres and L. C. Balbás, J. Phys. Condens. Matter **12**, 4365 (2000).
[34] R. Saito, G. Dresselhaus, M. S. Dresselhaus, *et al.*, *Physical properties of carbon nanotubes*, Vol. 35 (World Scientific, 1998).
[35] O. Gülseren, T. Yildirim, and S. Ciraci, Phys. Rev. B **65**, 153405 (2002).
[36] V. Barone, O. Hod, and G. E. Scuseria, Nano Lett. **6**, 2748 (2006).
[37] A. Rochefort, D. R. Salahub, and P. Avouris, J. Phys. Chem. B **103**, 641 (1999).
[38] N. Hamada, S.-i. Sawada, and A. Oshiyama, Phys. Rev. Lett. **68**, 1579 (1992).
[39] V. N. Popov, New J. Phys. **6**, 17 (2004).
[40] E. H. Lieb, Phys. Rev. Lett. **62**, 1201 (1989).
[41] S. Reich, C. Thomsen, and J. Maultzsch, *Carbon nanotubes: basic concepts and physical properties* (John Wiley & Sons, 2008).
[42] Y. Yin, P.-A. Hervieux, R. A. Jalabert, G. Manfredi, E. Maurat, and D. Weinmann, Phys. Rev. B **80**, 115416 (2009).